Electronic Supplementary Material (ESI) for ChemComm.

Supplementary materials

Dynamic single-site polysulfide immobilization in long-range disorder Cu-MOFs

Ju Sun[a], Xinxin Lu[a], Kuang-Hsu Wu[a], Jingwei Hou[c], Ruopian Fang[a], Judy N. Hart[d], Shenmin Zhu[e], Vicki Chen[c], Rose Amal[a], Da-Wei Wang[a,b*]

[a.] *Particles and Catalysis Research Laboratory, School of Chemical Engineering, The University of New South Wales, Sydney, NSW 2052, Australia*
[b.] *UNSW Digital Grid Futures Institute, The University of New South Wales, Sydney, NSW 2052, Australia*
[c.] *School of Chemical Engineering, University of Queensland, St. Lucia, Queensland, 4072, Australia*
[d.] *School of Materials Science and Engineering, The University of New South Wales, Sydney, NSW 2052 Australia*
[e.] *State Key Laboratory of Metal Matrix Composites, School of Materials Science and Engineering, Shanghai Jiao Tong University, Shanghai 200240 , China*

Experimental methods

Sample preparation

All the materials were used as received. The preparation of $Cu_3(BTC)_2$ follows the procedure reported by Ref[1,>. 1.2 g Benzene-1,3,5-tricarboxylic acid (H_3BTC, Sigma-Aldrich) was first dissolved in 20 ml ethanol (5 mmol) and sonicated for 1 min. 2.17 g $Cu(NO_3)_2$ (Sigma-Aldrich) was dissolved into 20 mL aqueous solution (9 mmol) and sonicated until totally dissolved. Later, H_3BTC solution was slowly added into $Cu(NO_3)_2$ solution with continuous stirring. The mixture solution was transferred into Teflon autoclave and heated under 180 C for 18 h. Later the product was collected and isolated by filtration three times. Afterwards, the blue crystal powder was dried under vacuum oven at 80 ºC overnight. Commercial nafion membrane 115 (Fuelcell Store) was received and cut into small round pieces with diameter of 17 mm. Then these membranes were put into aqueous NaOH solution (1 M) under 80 ºC for 16 h. Afterwards, in order to remove the residual salts, the membranes were rinsed by water several times and put into water under 80 ºC for 1 h again. The obtained nafion membranes were dried under vacuum oven at 80 ºC overnight.

Preparation of MOF/S and pure S cathode

The cathode was first prepared with sulfur, carbon black (CB, Sigma-Aldrich), and poly(vinylidene difluoride) (PVDF, Sigma-Aldrich) in a weight ratio of 8:1:1. Carbon coated aluminium foil (thickness, 10 mm in diameter, Sigma-Aldrich) was used as current collector. The sulfur cathode was heated under vacuum oven at 80 ºC for overnight and then taken out for the following coating. Sulfur loading for the cathode is 0.64 mg/cm^2. Another coating layer on the surface of sulfur cathode was $Cu_3(BTC)_2$, graphene and PVDF (ratio is 8:1:1). The cathode was transferred into vacuum oven at 80 ºC overnight. Sodium metal (Sigma-Aldrich) was employed as anode and cut into small round pieces with the diameter of 12 mm. Na anode was used as both counter and reference electrode.

Electrochemical measurement

Cell assembly was conducted in the argon-filled glove box. Sodiated nafion membrane was used as separator. 20 uL 1 M $NaCF_3SO_3$ in Triglyme as electrolyte was first dropped onto sulfur cathode, followed by the nafion membrane. Another 20 uL electrolyte was added on the separator and Na was put onto the separator. Cathode with pure S was also assembled as contrast test. The galvanostatic charge-discharge was tested using Land battery tester (CT2001A). The coin cell was cycled between the cut-off voltage of 1.2 V and 2.8 V at the current density of 0.2 C. The cyclic voltammetry (CV) and electrochemical impedance spectroscopy (EIS) were conducted by Biologic VSP potentiostat. CV test was investigated at a scan rate of 0.1 mV/s from 1.2 V to 2.8 V at room temperature.

Material Characterization

The morphology of $Cu_3(BTC)_2$ were obtained by scanning electron microscopy (SEM) via a FEI Nova NanoSEM 450 FE-SEM microscope at an accelerating voltage of 5 kV. The elemental mapping results were examined through an energy dispersive spectrometer (EDS) attached to the FEI Nova NanoSEM 450 FE-SEM. XRD pattern of cathode was collected by PANalytical Empyrean II diffractometer with Cu Kα radiation (λ = 0.15406 nm) at 45 kV and 40 mA. Before test, the sample was covered by a sample holder in the Ar-filled glove box. The X-ray photoelectron spectroscopic (XPS) technique was performed on a Thermo Scientific, UK (model ESCALAB250Xi) using Mg Kα (hν = 1486.68 eV) as the excitation source with 150W power (13 kV x 12 mA). MOF/S and pure sulfur cathode were first disassembled in the glove box, and washed by tetraethylene glycol dimethyl ether (TEGDME) solvent three times, dry under vacuum overnight. Then the samples were sealed and taken out for tests (XRD, XPS, SEM).

Ex-situ XANES and EXAFS studies

X-ray absorption fine structure (XAFS) was conducted at the BL17C1 beamline (a hard X-ray beamline) of Taiwan Light Source at National Synchrotron Radiation Research Center (NSRRC), Taiwan. XANES and EXAFS spectra at Cu K-edge were collected in fluorescence mode using a gas ionization chamber (Lytle) detector, taking Cu metal foil as the calibration standard. The energy intervals for pre-edge, near-edge and post-edge were set to be 2.0 eV, 0.5 eV and 0.05 eV, respectively. EXAFS data analysis and first-shell fitting were carried out using Athena and Artemis in Demeter Software Package>. The raw data were background-subtracted and normalized before Fourier-transform analysis using a k^3 weighting. The analysis and fitting followed the standard procedures as recommended for IFEFFIT[4]. No phase-correction was applied for the presenting data. The coordination number (CN) was calculated by the product of N (degeneracy) and s_0^2 amplitude as they are arithmetically inseparable and E_0 was kept at below 10 in absolute terms. An R-factor (goodness of fit) of < 0.02 has been satisfied in all fittings.

Computational details

Density Functional Theory (DFT) calculations were used to simulate the adsorption of Na^+, S^{2-} and Na_2S on a finite-size cluster model extracted from the crystalline structure of the metal-organic framework (MOF). The optimized bulk MOF was

employed to obtain the initial cluster model; a cluster of 62 atoms was extracted from the optimized bulk MOF, which consisted of a Cu^{2+} dimer and four BTC units (BTC = benzene-1,3,5-tricarboxylate). The carboxylates in the cluster were then saturated with H atoms. MOF metal nodes were considered as adsorption site, and thus the adsorbate species were placed near the Cu-O coordination site. Different adsorption configurations were optimized to understand the adsorption property of MOF. The calculations were conducted using the CRYSTAL17 DFT code> with the hybrid B3LYP exchange-correlation functional[6] and all-electron basis sets, specifically split-valence triple-ζ basis sets with polarisation functions (pob-TZVP basis sets for Cu, C and H[7] and a def2-TZVP basis set for O[8]). The SCF convergence threshold for the total electronic energy was set to 10^{-8} Hartree. The adsorption energies (E_{ads}) between the MOF cluster and adsorbate were calculated by:

$$E_{ads} = E_{total} - E_{MOF} - E_{adsorbate}$$

where E_{total} is the total energy of the optimized MOF cluster with the adsorbate (i.e. Na^+, S^{2-} or Na_2S), E_{MOF} is the energy of the optimized MOF cluster without adsorbate and $E_{adsorbate}$ is the energy of the isolated adsorbate species.

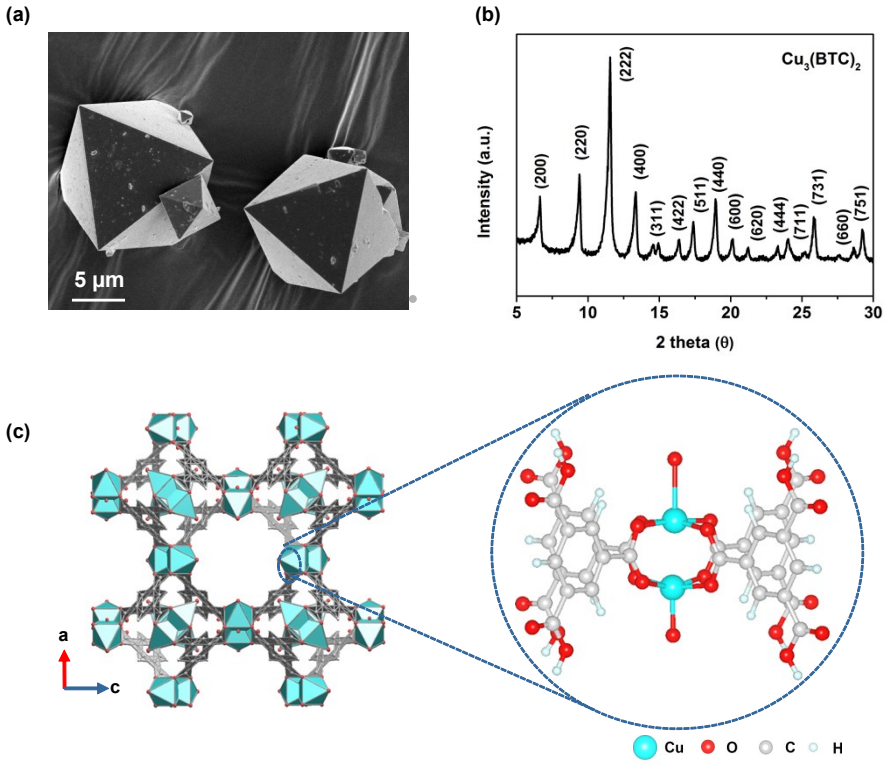

Fig. S1 a) SEM images of the pristine Cu-MOF particles. b) XRD spectra of ($Cu_3(BTC)_2$) powder. Crystalline structured $Cu_3(BTC)_2$ powder can be evidenced by (200), (220), (330), (400) phases. C) Crystal structure of Cu-MOF with Cu^{2+} dimers coordinated with four ligands. The square-planar Cu–O structure is shown in the enlarged picture.

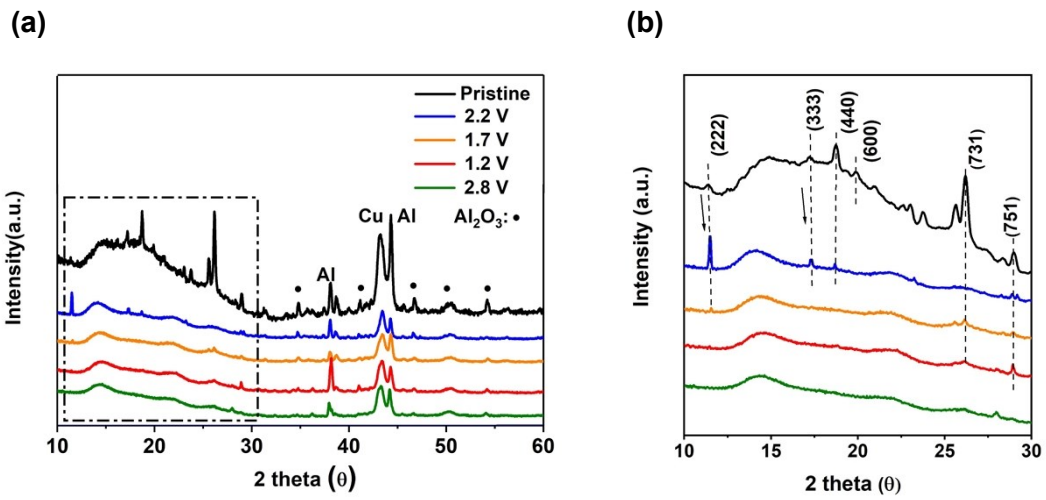

Fig. S2 Powder-XRD patterns of MOF/S cathodes at different electrochemical states, (b) The enlarged XRD spectra in the dotted box between the 2 theta range of 10 – 30° from a. Al peak in XRD figure is attributed to the Al current collector of the electrode; several Al2O3 peaks are due to the oxidation layer of Al foil. Cu arises from the sample holder. The humps at low 2θ around 14° are due to the Kapton foil which covers the material from moisture during XRD analysis. When Na-S cell is first discharged to 2.2 V, Cu-MOF particle partially keeps its original crystalline structure, of which (220), (330), (440) and (751) phases can be detected, but with significant loss in intensity. Its x-ray diffraction peaks nearly vanished when being discharged to 1.7 V. Furthermore, no crystalline signal is found after being discharged to 1.2 V or charged back to 2.8 V, demonstrating that the crystalline structure of MOF is vanished and the amorphization of the Cu-MOF is irreversible.

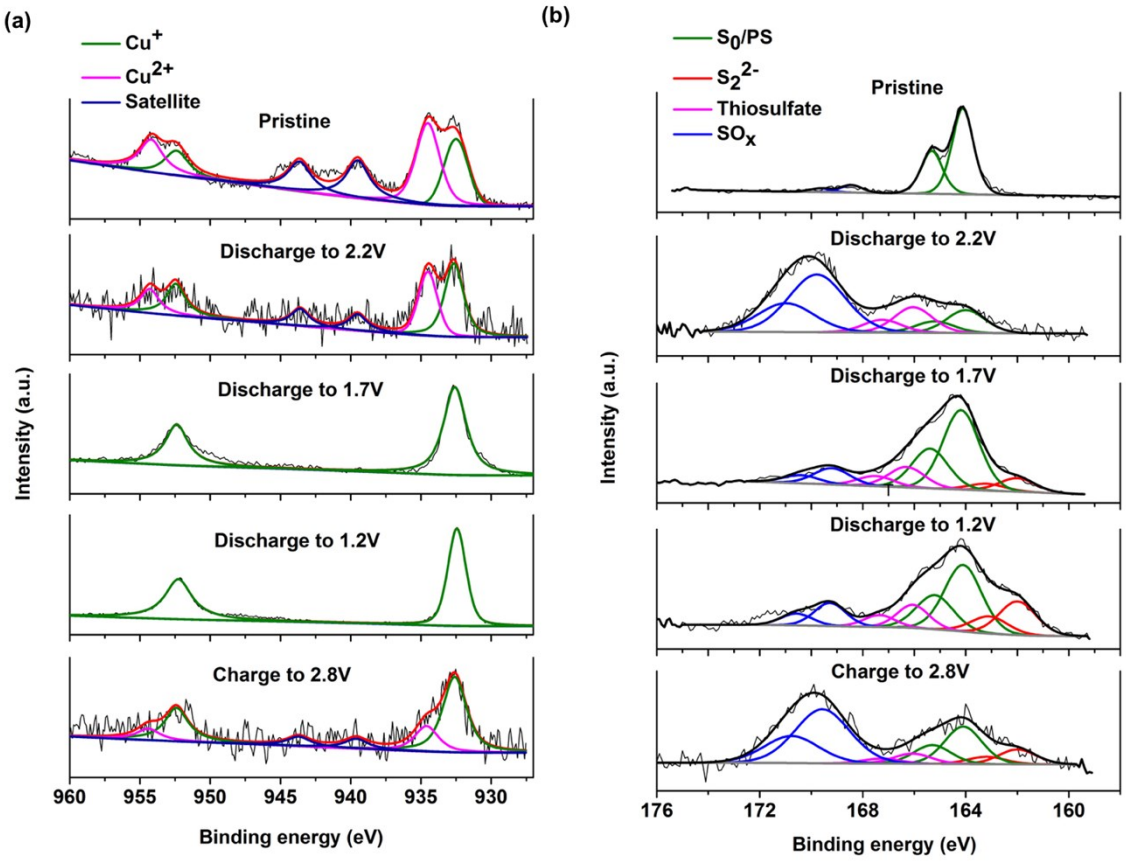

Fig. S3 *Ex-situ* XPS spectra of Cu-MOF cathodes after different electrochemical states (a) Cu 2p; (b) S 2p. XPS analysis of Cu 2p was first applied on the cathodes after galvanostatic cycling at different electrochemical states. For the pristine one, distinct peaks Cu 2p 3/2 were shown and can be split into two subordinate peaks, namely Cu^{2+} centered at 934 eV and Cu^{+} at 932.5 eV. A series of shake-up satellites ranges between 939 eV and 945 eV are the evidence of Cu^{2+} state[9,1]>. Basically, Cu^{+} is linked to the chemical Cu_2O and Cu^{2+} to CuO, $(-COO)_2Cu$, and Cu-epoxy complexes as well, which located in the coordination to the Cu centers BTC ligands[11]. When the battery was discharged to 2.2 V, the ratio of Cu^{2+}/Cu^{+} decreased as compared with the pristine one, and Cu^{2+} peak signal disappeared when discharged to 1.2 V. Cu^{2+} signal appeared again at 2.8 V and suggested the restoration of Cu-O bond in $Cu_3(BTC)_2$ structure. The cell was reduced to 1.2 V at cut-off voltage, with the occurrence of S^{2-}/S_2^{2-} at 119. 8 V, which can explain the strong interaction between Cu^{+} and polysulfides.

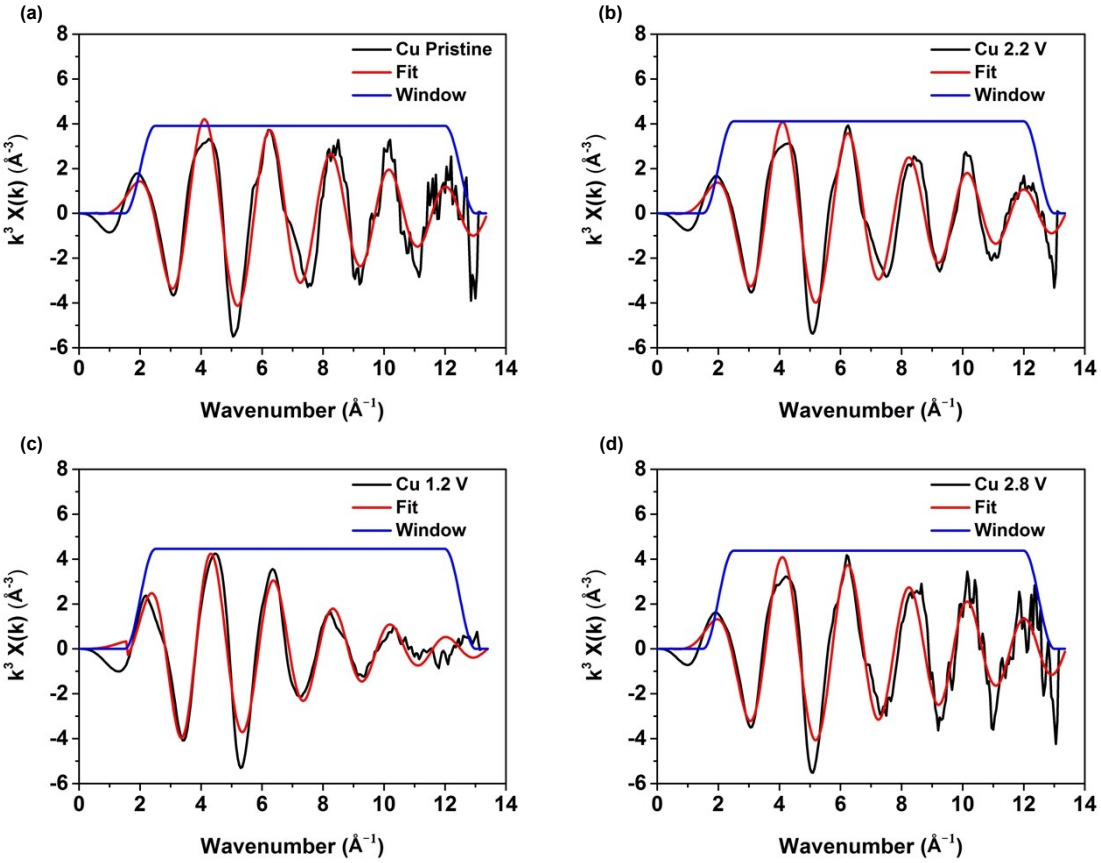

Fig. S4 First shell Fitted k^3-weighted *x(k)* functions of Cu-MOF cathodes for different electrochemical states

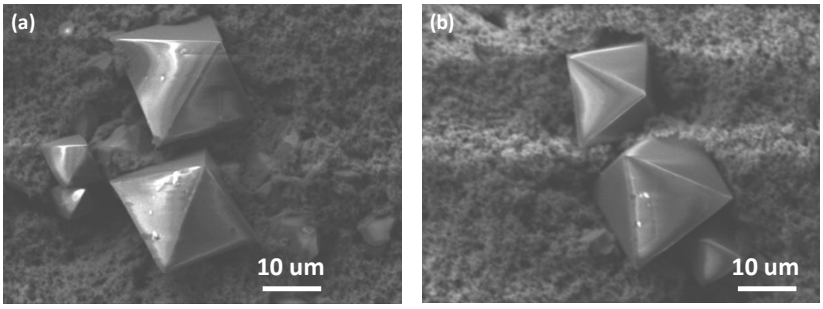

Fig. S5 SEM images of Cu-MOF electrodes after cycled at 2 C for 10 cycles, (a) after discharged to 1.2 V; (b) after charged to 2.8 V

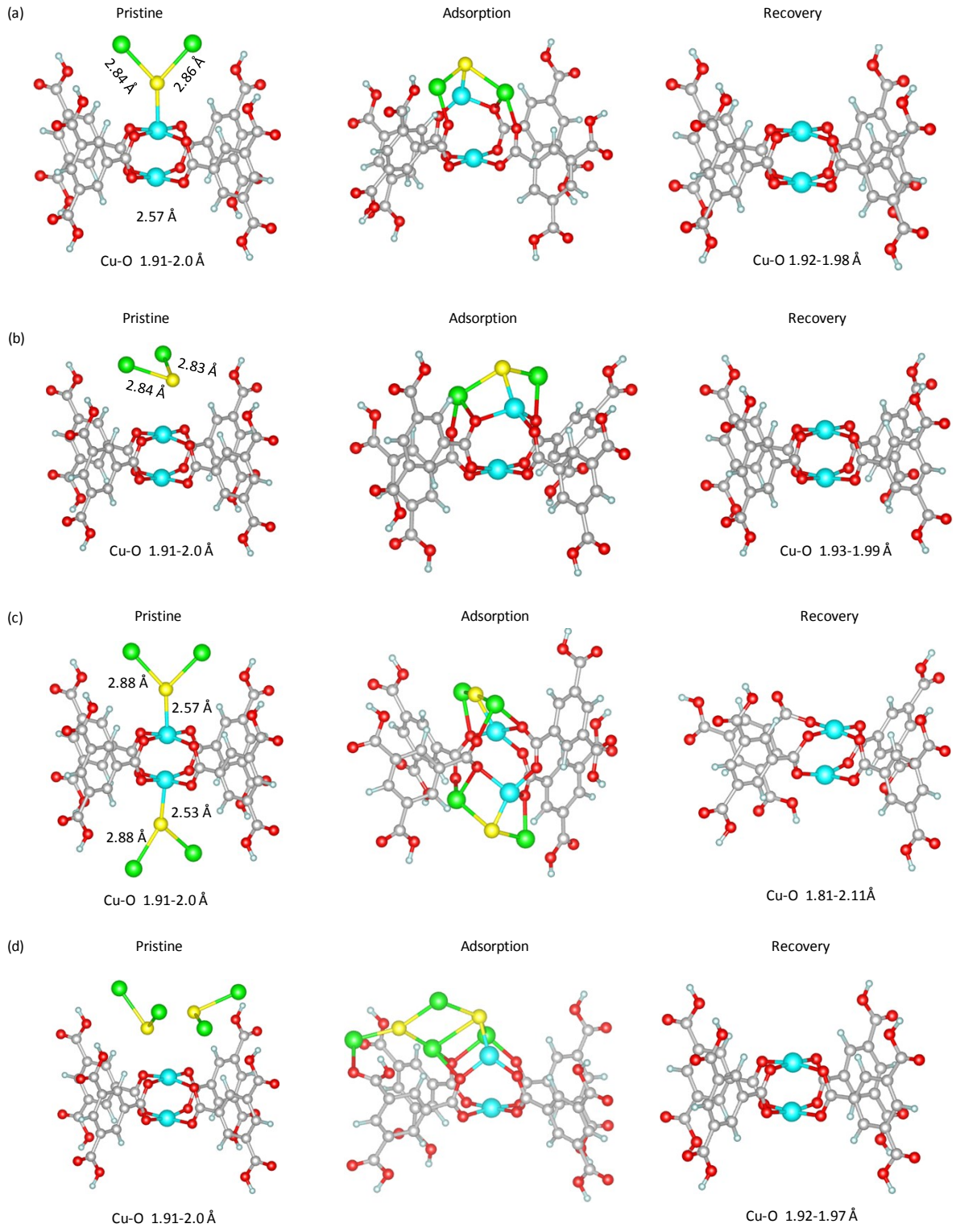

Fig. S6 DFT calculations for Cu-MOF materials adsorbing Na_2S in different ways. Configurations of a variety of Cu-MOF clusters absorbing Na_2S are displayed in Fig. S6. Single/double Na_2S molecules with different locating places were demonstrated as above, and these sulfides were adsorbed on distorted Cu-MOF clusters to form different configurations. The Cu-MOF clusters can be restored back with similar Cu-O bond length as the pristine one after charge back to 2.8 V.

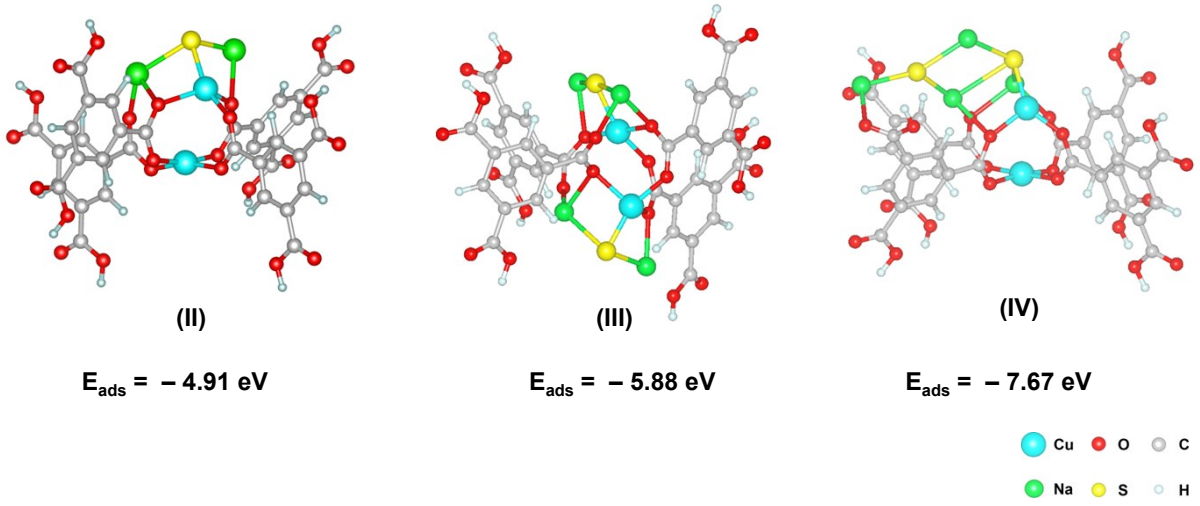

Fig. S7 Different adsorption configurations (II, III, IV) from Na_2S molecules attached to Cu sites when at 1.2 V, with adsorption energy of –4.91 eV, –5.88 eV and –7.67 eV, respectively.

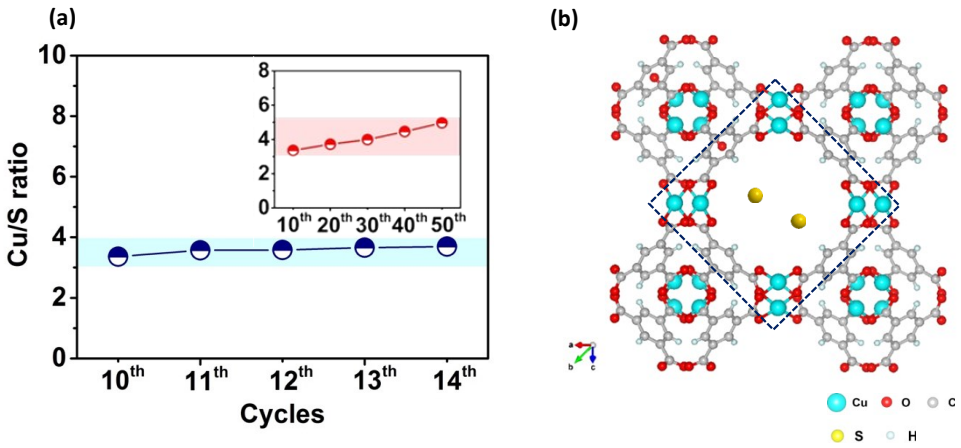

Fig. S8 Reversibility and ion accessibility of Cu-MOF. A) Cu/S ratio in MOF for Na-S batteries cycled between 10^{th} – 14^{th} cycles, inset is the Cu/S values at 10^{th}, 20^{th}, 30^{th}, 40^{th} and 50^{th} cycle. b) structural illustration of sulfur utilization versus Cu atoms in the MOF.

Tab. S1 Fitted summary of Cu-MOF cathodes derived from EXAFS fitting

Parameters	**Cu-Pristine**	**Cu-2.2V**	**Cu-1.2V**	**Cu-2.8V**
CN	3.21 ±0.27	3.18 ±0.29	3.07 ±0.35	3.20 ±0.30
R	1.973 ±0.010Å	1.974 ±0.011Å	1.985 ±0.016Å	1.973 ±0.005Å
Sigma2	0.00515	0.00547	0.00790	0.00535
R-factor	0.0116	0.01294	0.0187	0.01952

Supplementary References

1 A. Aarti, S. Bhadauria, A. Nanoti, S. Dasgupta, S. Divekar, P. Gupta and R. Chauhan, *RSC Adv.*, 2016, **6**, 93003–93009.

2 P. C. Lemaire, J. Zhao, P. S. Williams, H. J. Walls, S. D. Shepherd, M. D. Losego, G. W. Peterson and G. N. Parsons, *ACS Appl. Mater. Interfaces*, 2016, **8**, 9514–9522.

3 B. Ravel and M. Newville, *J. Synchrotron Radiat.*, 2005, **12**, 537–541.

4 M. Newville, *J. Synchrotron Radiat.*, 2001, **8**, 322–324.

5 R. Dovesi, A. Erba, R. Orlando, C. M. Zicovich-Wilson, B. Civalleri, L. Maschio, M. Rérat, S. Casassa, J. Baima, S. Salustro and B. Kirtman, *Wiley Interdiscip. Rev. Comput. Mol. Sci.*, 2018, **8**, 1–36.

6 I. D. Petsalakis, G. Theodorakopoulos and J. Whitten, *Phys. Chem. Chem. Phys.*, 2015, **17**, 428–433.

7 M. F. Peintinger, D. V. Oliveira and T. Bredow, *J. Comput. Chem.*, 2013, **34**, 451–459.

8 P. Pernot, B. Civalleri, D. Presti and A. Savin, *J. Phys. Chem. A*, 2015, **119**, 5288–5304.

9 M. Yin, C.-K. Wu, Y. Lou, C. Burda, J. T. Koberstein, Y. Zhu and S. O'Brien, *J. Am. Chem. Soc.*, 2005, **127**, 9506–9511.

10 F. Han, W. C. Li, D. Li and A. H. Lu, *ChemElectroChem*, 2014, **1**, 733–740.

11 N. A. Travlou, K. Singh, E. Rodríguez-Castellón and T. J. Bandosz, *J. Mater. Chem. A*, 2015, **3**, 11417–11429.